Novel Liquid Crystalline Block Copolymers by ATRP and ROMP

Min-Hui Li,*† Patrick Keller,† and Pierre-Antoine Albouy‡

Laboratoire Physico-Chimie Curie, UMR168 CNRS, Institut Curie, 11 Rue P. & M. Curie, 75231 Paris Cedex 05, France, and Laboratorie de Physique des Solides, UMR8502 CNRS, Université Paris-Sud, 91405 Orsay Cedex, France

Received September 12, 2002; Revised Manuscript Received January 10, 2003

ABSTRACT: Two new liquid crystalline block copolymers have been synthesized: a side-on liquid crystalline/isotropic (LC/Iso) triblock copolymer **ABA** (**B** = LC) by ATRP and a side-on LC/Iso diblock copolymer **AB′** (**B′** = LC) by first synthesizing the LC block (**B′**) using ROMP and then the Iso block using ATRP. Absolute values of molar masses of the homopolymers and of the block copolymers were determined using SEC with an on-line light-scattering instrument: $M_n = 1.43 \times 10^4$, $M_w/M_n = 1.04$ for homopolymer **B**, $M_n = 3.47 \times 10^4$, $M_w/M_n = 1.32$ for triblock copolymer **ABA**, $M_n = 2.29 \times 10^4$, $M_w/M_n = 1.06$ for homopolymer **B′**, and $M_n = 3.61 \times 10^4$, $M_w/M_n = 1.28$ for diblock copolymer **AB′**. The di and triblock copolymers self-assemble into lamellar mesophases in which the LC blocks undergo transitions similar to those of the homopolymers. Lamellar structures were studied as a function of temperature by polarized optical microscopy, DSC and X-ray diffraction. Those new liquid crystalline block copolymers could be used as model systems for "artificial muscles".

Introduction

Hybrid liquid crystalline/isotropic (LC/Iso) block copolymers are attractive candidates for the development of new functional materials, such as smart or responsive materials and electrooptical systems, because the block copolymers tend to self-assemble into ordered micrometer- or nanometer-sized domains, while special functions can be introduced via the LC parts into the micro- or nanostructure of the block copolymers. Our work is motivated by the possibility of realizing an artificial muscle or actuator from an isotropic/nematic/isotropic (Iso/N/Iso) triblock copolymer as proposed recently by de Gennes.[1] The Iso/N/Iso block copolymer should first self-assemble into an oriented lamellar structure in which the mesogenic units must be homogeneously aligned throughout the whole sample. Then the amorphous layers should be cross-linked to form an elastomer. In the nematic state, the LC block chain conformation will be elongated along the nematic director axis, while in the isotropic state it will recover an isotropic random conformation.[2,3] As a result, a reversible contraction and expansion of the elastomer will take place when the LC block undergoes the nematic ↔ isotropic phase transition.

The synthesis of block copolymers with well-defined structures and narrow molecular-weight distributions is a crucial step for the realization of this material, because only block copolymers with a narrow molecular-weight distribution of each of their components will display very regular, long-range ordered structures. In the Iso/N/Iso system proposed by de Gennes, the nematic block is a main-chain LC polymer. However, due to the polycondensation reactions used for the synthesis, most main-chain LC polymers exhibit fairly large polydispersities. In contrast, the polymerizations used to prepare side-chain LC polymers allow the synthesis of macromolecules with narrow molecular weight distributions. For one class of side-chain LC polymer, the side-on nematic polymers, structural studies[4,5] demonstrated that its conformational behavior was similar to the that of main-chain LC polymers. In the nematic phase, the backbone is strongly elongated in the direction of the nematic director due to the strong coupling between the liquid crystalline order and the chain conformation. Recently, a musclelike material has been realized using this kind of side-on nematic homopolymer.[6] Therefore, we chose side-on LC polymers to construct the LC domain in block copolymers with the aim of realizing an artificial muscle.

There are two main strategies to prepare well-defined side-chain LC/Iso block copolymers (for review, see refs 7−10). The first one uses sequential living or controlled polymerization of the LC and Iso monomers, including anionic,[11−14] cationic,[15] ring-opening metathesis (ROMP),[16] or group transfer polymerizations.[17] The second uses polymer-analogous reactions to introduce the mesogenic groups onto conventional pre-block copolymers.[18−22] Recently, the controlled ("living") radical polymerizations of nitroxide-mediated radical polymerization[23−25] and atom transfer radical polymerization (ATRP),[26−29] have been used to synthesize LC side chain polymers. Among these works, two attempts have been made to synthesize LC/Iso diblock copolymers by nitroxide-mediated radical polymerization.[23,24] Compared to the other living methods, these controlled radical polymerizations have some benefits: the number of monomers that can be (co)polymerized is quite extensive, and the reactions are not water sensitive and do not require ultrapure solvents and reagents. ATRP is of particular interest, since it is applicable to both styrenic and (meth)acrylate monomers and is remarkably tolerant of functional groups. In a previous paper,[29] we reported LC side-chain homopolymers prepared by ATRP. Here we present the synthesis of a side-on Iso/LC/Iso triblock copolymer by ATRP and a side-on LC/Iso diblock copolymer by a combination of ROMP and ATRP (Figure 1). The mesomorphic properties and self-assembly structures created by these new block copolymers will also be discussed.

* Corresponding author. E-mail: min-hui.li@curie.fr.
† Institut Curie.
‡ Université Paris-Sud.

10.1021/ma021473o CCC: $25.00
Published on Web 03/13/2003

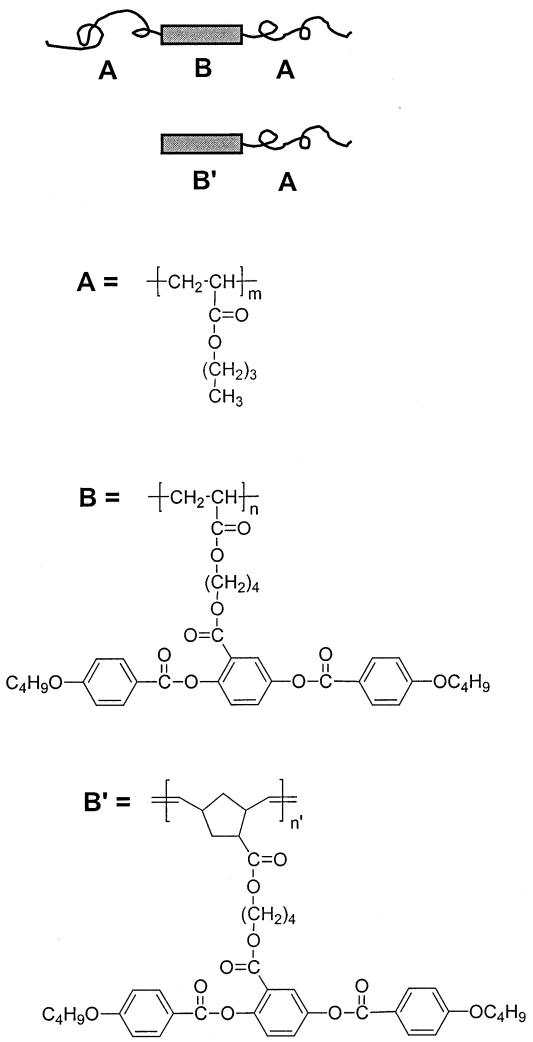

Figure 1. Chemical structures of the block copolymers **ABA** and **AB′**.

Experimental Section

1. Materials. $Cu^{I}Br$ (98%, Aldrich) and $Cu^{I}Cl$ (98%, Aldrich) were purified as previously described.[30] 4,4′-Di(*n*-nonyl)-2,2′-bipyridine (bpy9) was synthesized according to reported procedures.[31,32] Diethyl *meso*-2,5-dibromoadipate (98%, Acros) was used without further purification. *n*-Butyl acrylate (*n*-BA) (99%, Aldrich) was filtered from neutral Al_2O_3 before use. Grubbs' ruthenium initiator was used as received from Strem (Figure 2). CH_2Cl_2 (analytical purity) was treated with CaH_2 and distilled under argon. The syntheses of the monomer **A444** (Figure 2) was described in ref 6. The preparation of the monomer **NB444** (Figure 2) was the same with that of the side-on acrylate monomers reported in ref 33, except the last step. In the preparation of **NB444**, the mesogen with the alcohol-containing spacer was reacted with *exo*-5-norbornene-2-carboxylic acid in the last step.

2. Triblock Copolymer Synthesis by ATRP.[34] A. Difunctional Polymerization of A444. $Cu^{I}Br$ (7.18 mg, 0.05 mmol), $Cu^{II}Br_2$ (0.56 mg, 0.0025 mmol), diethyl *meso*-2,5-dibromoadipate (36 mg, 0.1 mmol), bpy9 (42.84 mg, 0.105 mmol), and monomer **A444** (2.528 g, 4 mmol) were added into a Schlenk flask. The flask was degassed by four vacuum−argon cycles. Toluene (2.5 mL), which was previously degassed by bubbling argon through it for 30 min, was then introduced into the flask using a syringe purged with argon. The flask was then placed in an oil bath thermostated at 80 °C. With the progressive solubilization of $Cu^{I}Br$, the solution became brown (10−20 min). The reaction solution was stirred at 80 °C for 49 h. The resulting polymer solution was poured into a large volume of diethyl ether. The precipitated polymer **PA444** was purified 4 times by dissolution in a small amount of acetone and precipitation into a large volume of diethyl ether (volume ratio of diethyl ether/acetone was 50/3). The white polymer was dried under vacuum at room temperature for 3 days; yield 1.32 g (52%). The polymer had a $M_n = 1.53 \times 10^4$ (degree of polymerization = 24) and a $M_w/M_n = 1.04$.

B. Block Copolymerization of *n*-BA with Difunctional PA444 as Macroinitiator. $Cu^{I}Cl$ (1.88 mg, 0.019 mmol), bpy9 (15.47 mg, 0.038 mmol), and **PA444** (0.145 g, 0.0095 mmol) were added into a Schlenk flask. The flask was degassed by four vacuum−argon cycles. *n*-Butyl acrylate (0.3 mL, 2.09 mmol) and toluene (0.2 mL), which were previously degassed by bubbling argon through them for 30 min, were then introduced into the flask using syringes purged with argon. The reaction solution was stirred at 80 °C for 24 h. The resulting polymer solution was poured into a large volume of methanol. The precipitated polymer **ABA** was purified three times by dissolution in a small amount of toluene and precipitation into a large volume of methanol (volume ratio of methanol/toluene was 50/3). The sticky polymer was dried under vacuum at room temperature for 3 days; yield 0.32 g (68%). The triblock copolymer had a $M_n = 3.47 \times 10^4$ (weight ratio of LC block on Iso block is 42/58) and a $M_w/M_n = 1.32$.

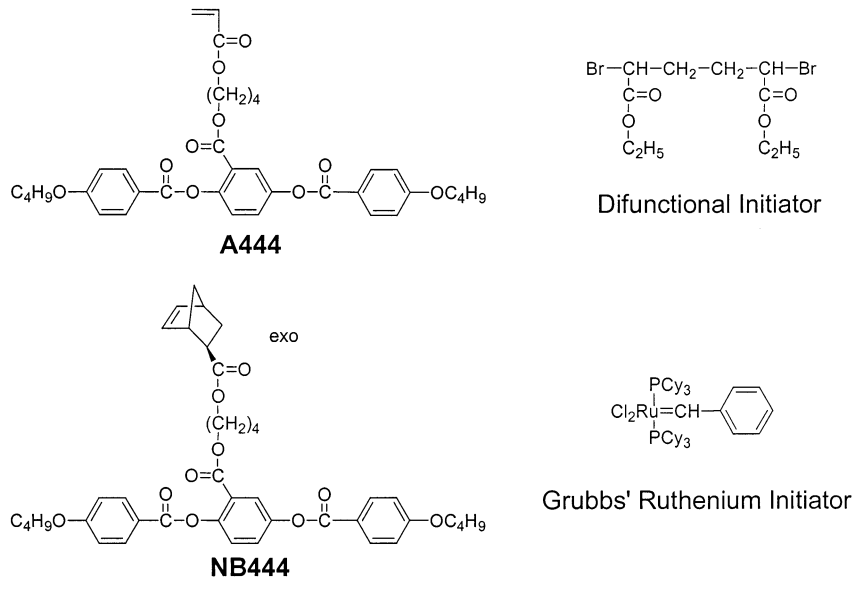

Figure 2. LC monomers and initiators.

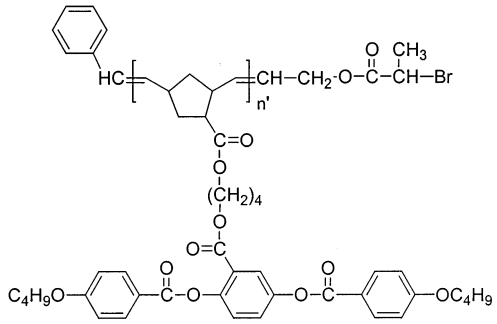

Figure 3. Monofunctional LC polymer **PNB444**.

3. Diblock Copolymer Synthesis by ROMP and ATRP. A. NB444 Polymerization by ROMP and Monofunctionalization of PNB444 (Figure 3). The *exo*-norbornene monomer **NB444** (400.43 mg, 0.57 mmol) and the Grubbs' ruthenium initiator (18.46 mg, 0.022 mol) were placed in a Schlenk flask equipped with a septum and connected to a vacuum line. The Schlenk flask was flushed with argon for 15 min. Under a small positive argon pressure, 4 mL of distilled and argon-degassed dichloromethane was added via syringe.

The reaction solution was stirred under argon for 3 h. Then, was added via syringe 250 μL (1.1 mmol) of the termination reagent (4-(2-bromopropionyloxy)-but-2-enyl 2-bromopropionate). The color of the solution changed from light pink to orange-brown immediately. The reaction solution was stirred for 1 h, then poured into a large volume of methanol (40 mL). The precipitated polymer **PNB444** (Figure 3) was purified three times by dissolution in a minimum volume of dichloromethane and precipitation into a large volume of methanol (volume ratio of methanol/dichloromethane was 40/4). The white polymer was dried under vacuum for 3 days; yield 0.36 g (90%). The polymer had a $M_n = 2.29 \times 10^4$ (degree of polymerization = 33) and a $M_w/M_n = 1.06$.

B. Block Copolymerization of *n*-BA by ATRP with Monofunctional PNB444. Cu^ICl (1.29 mg, 0.013 mmol), bpy9 (10.92 mg, 0.027 mmol) and **PNB444** (0.150 g, 0.0065 mmol) were added into a Schlenk flask. The flask was degassed by four vacuum−argon cycles. *n*-Butyl acrylate (0.3 mL, 2.09 mol) and toluene (0.2 mL), which were previously degassed by bubbling argon through them for 30 min, were then introduced into the flask using syringes purged with argon. The reaction solution was stirred at 80 °C for 44 h. The resulting polymer solution was poured into a large volume of methanol. The precipitated polymer **AB′** was purified three times by dissolution in a small amount of toluene and precipitation into a large volume of methanol (volume ratio of methanol/toluene was 50/3). The sticky polymer was dried under vacuum at room temperature for 3 days; yield 0.24 g (34%). The diblock copolymer had a $M_n = 3.61 \times 10^4$ (weight ratio of the LC block on the Iso block is 58/42) and a $M_w/M_n = 1.28$.

4. Characterization. The mesomorphic properties were studied by thermal optical polarizing microscopy using a Leitz Ortholux microscope equipped with a Mettler FP82 hot stage, and differential scanning calorimetry using a Perkin-Elmer DSC7. The DSC7 instrument was calibrated with a Perkin-Elmer indium calibration kit (mp, 429.78 K (156.60 °C); ΔH, 6.80 cal·g^{-1}) for temperature and enthalpy changes. The heating and cooling rates were 10 °C·min^{-1}.

The molecular weights and the molecular weight distributions were measured by size exclusion chromatography (SEC) using Waters Styragel HR 5E columns, a Waters 410 differential refractometer, and a Waters 486 UV detector, on line with a Wyatt miniDAWN light scattering instrument. With the used columns, the molecular weight range claimed to separate is 2×10^3 to 4×10^6 of PS equivalent. The light wavelength of the differential refractometer is 930 nm and that of the light scattering detector 690 nm. THF was used as the eluent at 1 mL/min. The differential refractive index increment dn/dc was measured separately on the same refractometer (at $T = 40$ °C) for LC homopolymers.

Using Wyatt miniDAWN light scattering instrument on line with SEC, the molar mass M_i of the polymers in each volume slice of the chromatogram (e.g., in the ith slice) is calculated as follows[35]

$$M_i = \left[\frac{k(\mathrm{d}n/\mathrm{d}c)_i \Delta n_i}{R_{0_i}}\right]^{-1} \tag{1}$$

where R_{0i} is the excess Rayleigh ratio (cm^{-1}) of the polymer solution in ith slice compared to that of the solvent alone at scattering angle $\theta = 0$, using a vertically polarized incident light. k is an optical constant. $(dn/\mathrm{d}c)_i$ is the differential refractive index increment of the polymer solution in the ith slice with respect to a change in polymer concentration, expressed in mL·g^{-1}. Δn_i is the change in refractive index of the ith slice compared to pure solvent measured by the differential refractometer.

The polymer concentration in the ith slice is

$$c_i = \Delta n_i (\mathrm{d}n/\mathrm{d}c)_i^{-1} \tag{2}$$

The average molar masses M_n and M_w of the polymer sample can be obtained using eqs 1 and 2 as follows:

$$M_w = \frac{\sum (c_i M_i)}{\sum c_i} \tag{3}$$

$$M_n = \frac{\sum c_i}{\sum \frac{c_i}{M_i}} \tag{4}$$

In the case of the LC homopolymers, $dn/\mathrm{d}c$ is a constant for all slices and is measured beforehand by the differential refractometer: $(dn/\mathrm{d}c)_i \equiv dn/\mathrm{d}c = 0.156$ for **PA444** and $(dn/\mathrm{d}c)_i \equiv dn/\mathrm{d}c = 0.157$ for **PNB444**. The absolute values of M_n and M_w of the LC homopolymers were thus determined by the light-scattering method.

However, in the case of the LC/Iso block copolymers, dn/dc is a variable for each slice because it is a function of the relative composition of the blocks or the molar mass. In our calculation, 100% mass recovery was then assumed

$$W_{\text{injected}} = \sum v c_i = v \sum c_i \tag{5}$$

and a mean value of $dn/\mathrm{d}c$ was deduced

$$\overline{\mathrm{d}n/\mathrm{d}c} = \frac{v \sum \Delta n_i}{W_{\text{injected}}} \tag{6}$$

where W_{injected} is the total injected weight of the polymer sample and v the volume of each slice.

Using this mean value $\overline{\mathrm{d}n/\mathrm{d}c}$ for each slice, the values of M_n and M_w obtained could be wrong, since M_n and M_w might depend on $(\mathrm{d}n/\mathrm{d}c)_i$. Using relations 1, 2, and 5, eqs 3 and 4 can be written as

$$M_w = \frac{\sum (c_i M_i)}{\sum c_i} = \frac{v \sum [(\mathrm{d}n/\mathrm{d}c)_i^{-2} R_{0i}]}{k W_{\text{injected}}} \tag{7}$$

$$M_n = \frac{\sum c_i}{\sum \frac{c_i}{M_i}} = \frac{W_{\text{injected}}}{vk \sum \frac{\Delta n_i^2}{R_{0i}}} \tag{8}$$

M_n thus measured does not depend on $(\mathrm{d}n/\mathrm{d}c)_i$, but M_w does depend on $(\mathrm{d}n/\mathrm{d}c)_i$. So only M_n of the block copolymer measured here by light scattering on line with SEC is correct. The value

of M_w of the block copolymer was then evaluated as follows

$$M_w = M_n\left(\frac{M_w}{M_n}\right) \quad (9)$$

where M_n was obtained by light scattering and M_w/M_n by calibration method with a PS standard.

The value of M_w/M_n of the block copolymer is considered as "equal" to its PS-equivalent M_w/M_n value with a reasonable approximation (for detail, see Supporting Information).

5. Structural Study by X-ray Scattering. The X-ray scattering experiments were performed on samples contained in glass capillaries (1 mm diameter) using Cu Kα radiation (λ = 1.54 Å) from a 1.5 kW rotating anode generator. WAXS and SAXS were performed separately. In the case of the diblock copolymer, only powder samples were studied. In the case of the triblock copolymer, both powder samples and aligned samples were studied. The alignment was obtained by slowly cooling (0.1°C·min^{-1}) the sample in a magnetic field (1.7 T) from the isotropic phase to room temperature. The X-ray experiments on aligned samples were then made at room temperature. SAXS on powder samples was performed in an oven at different temperatures; the samples were first heated once to isotropic phase before any SAXS experiments. The diffraction patterns were recorded on photosensitive imaging plates.

Results and Discussion

1. Molecular Weights, Molecular Weight Distributions, and Compositions of Block Copolymers. The SEC chromatograms of the LC homopolymers and of the corresponding block copolymers are shown in Figure 4. The values of M_n and of M_w/M_n are also given. The success of the copolymerization is clearly shown by the shift of the peak position of the block copolymer toward high molecular mass side in each figure. Light scattering on line with SEC was used to analyze the molecular weights. If a conventional calibration method had been used, M_n would have had a large error because the molecular weight of the monomer is very high (typically 600 g mol^{-1}) and the chemical structure of the polymer is very different compared to those of usual narrow molecular weight standards (e.g., polystyrene). Using the light-scattering method, we obtained the absolute values of M_n and M_w directly for the homopolymers, but only M_n for the block copolymers, because the differential refractive index increment (d*n*/d*c*) of the polymer solution required by light-scattering method is a function of the copolymer composition or the molecular weight itself (see section 4, Characterization). For example, the value of M_w/M_n determined directly by light scattering is 1.08 for the triblock copolymer, which is very close to that of the homopolymer (1.04). Nevertheless, the chromatogram peak of the triblock copolymer is significantly broader than that of the homopolymer (Figure 4). So, the M_w as well as M_w/M_n measured by light scattering on line with SEC are questionable (see section 4, Characterization). The conventional calibration method with polystyrene stardards was then used to evaluate M_w/M_n (Supporting Information). The value of M_w/M_n for the triblock copolymer thus determined is 1.32, which might be closer to reality than the value of 1.08 measured by light scattering. The value of M_w of the copolymer can be then obtained by eq 9 using M_n obtained by light scattering and M_w/M_n by calibration method with PS standard.

The molecular weights and molecular weight distributions for all the polymers studied are summarized in Table 1.

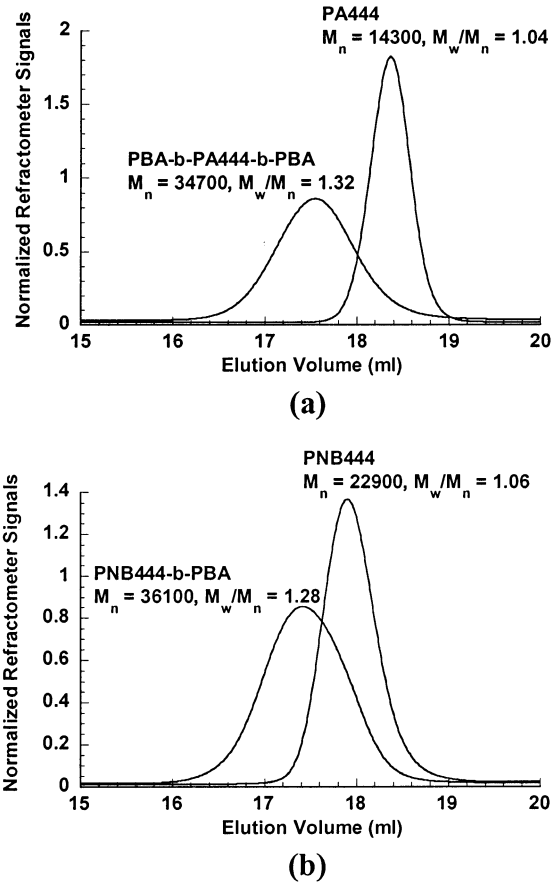

Figure 4. SEC chromatograms: (a) of the LC homopolymer **PA444** and the triblock copolymer **ABA** (**PBA-*b*-PA444-*b*-PBA**); (b) of the LC homopolymer **PNB444** and the diblock copolymer **AB′** (**PNB444-*b*-PBA**). The refractometer signals were normalized with respect to the peak area.

Table 1. Molecular Weights, Molecular Weight Distributions, and Compositions of the Polymers Studied

polymer	M_n[a]	M_w	M_w/M_n	x_B or $x_{B'}$
PA444	1.53×10^4	1.59×10^4 [a]	1.04[a]	1
PNB444	2.29×10^4	2.43×10^4 [a]	1.06[a]	1
PBA-*b*-PA444-*b*-PBA	3.47×10^4	4.58×10^4 [c]	1.32[b]	0.42[d]
PNB444-*b*-PBA	3.61×10^4	4.62×10^4 [c]	1.28[b]	0.58[d]

[a] The values were measured by light scattering method on line with SEC. [b] The values were PS-equivalent ones measured by conventional calibration method. [c] $M_w = M_n(M_w/M_n)$. [d] x_B or $x_{B'}$, the average weight ratio of LC block as measured by UV detector. It is equal to the peak area of the block copolymer divided by the peak area of the LC homopolymer with the same injected weight, because only the LC block in the copolymer gave UV signals.

2. Mesomorphic Properties and Self-Assembled Structures. LC homopolymers **PA444** and **PNB444** are nematic. They show typical Schlieren textures under a polarizing microscope (Supporting Information). However, triblock and diblock LC/Iso copolymers prepared with these components show typical smectic-like textures (Figure 5). In the block copolymers, two distinct levels of organization are taking place: the supramolecular lamellar structure due to the segregation between LC and Iso blocks and the molecular nematic structure in the LC sublayers. Figures 6 and 7 show, respectively, SAXS and WAXS patterns of an aligned triblock copolymer sample at room temperature. The magnetic field **H** was perpendicular to the capillary axis and the incident X-ray was perpendicular to both of them. An oriented lamellar structure with a 17.2 nm

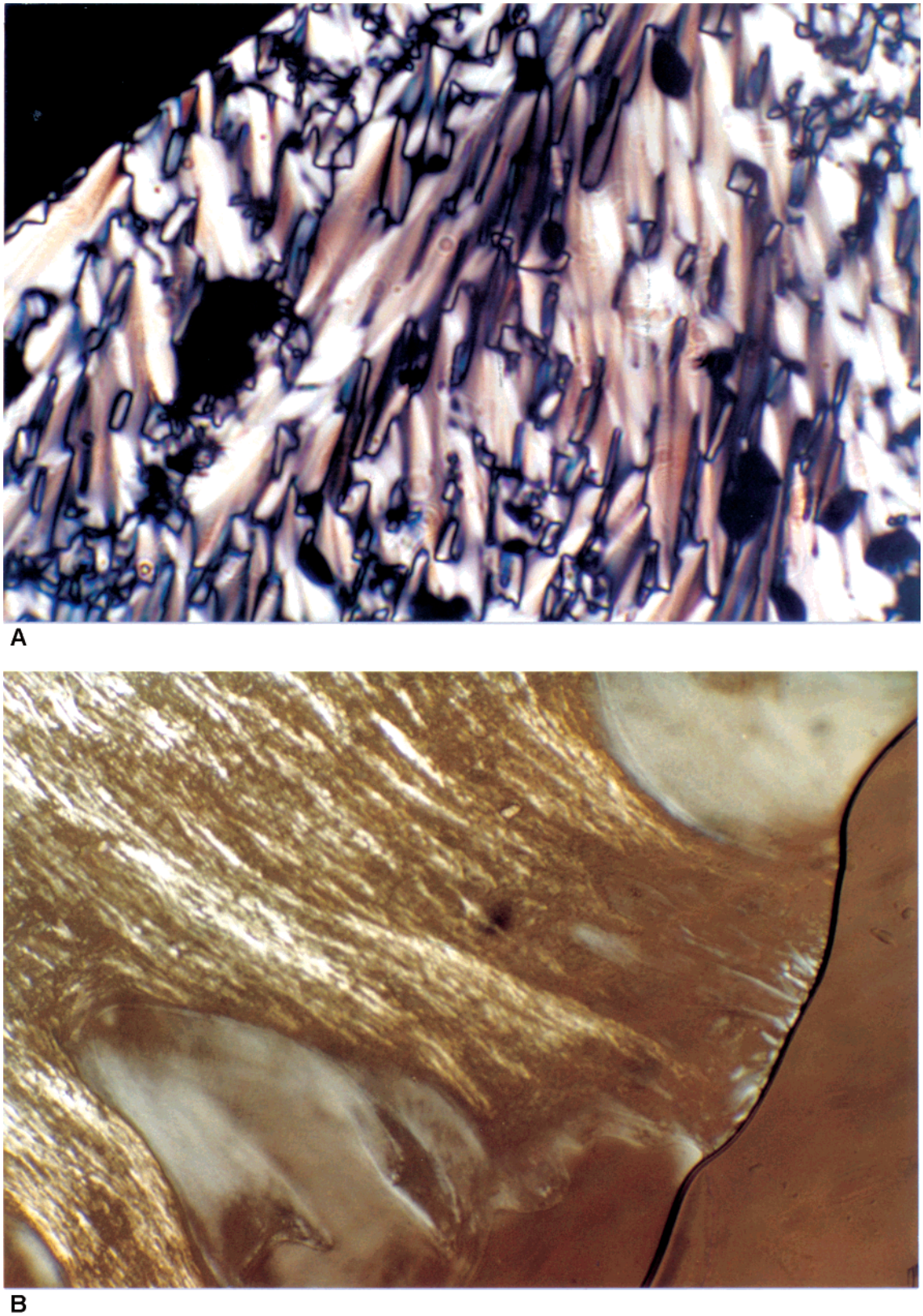

Figure 5. Textures of the supramolecular lamellar phases under polarizing microscope: (a) triblock copolymer **ABA** at 85.3 °C; (b) diblock copolymer **AB′** at 102.9 °C.

layer thickness is demonstrated by Figure 6. The layer normal is parallel to the magnetic field **H.** The degree of parallelism of the lamella related to the capillary axis is $10 \pm 1°$, which was evaluated from the angular profile of the diffraction signals. From WAXS (Figure 7), the lateral distance between mesogens in the nematic sublayer appears as a broad peak in the range 0.4−0.5 nm whose average is 0.44 nm. There is a slight anisotropy of the broad circle along the equator. The analysis of the angular profile of the broad circle shows that the LC sublayer is not homogeneously aligned. Some mesogens are aligned along the magnetic field **H** (as the supramolecular layer normal) with a nematic order parameter $S = 0.53 \pm 0.05$ (according to the approach

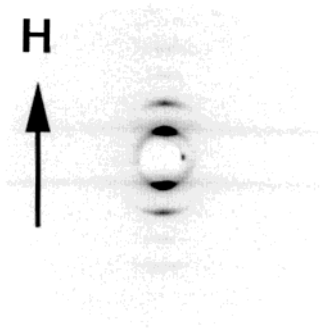

Figure 6. SAXS pattern of an aligned sample of the triblock copolymer **ABA** at room temperature. **H** is the direction of the applied magnetic field.

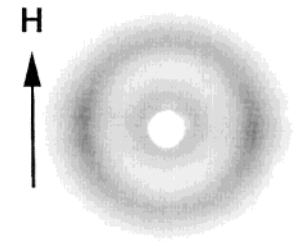

Figure 7. WAXS pattern of an aligned sample of the triblock copolymer **ABA** at room temperature. **H** is the direction of the applied magnetic field.

described in ref 36), while the remaining part is not aligned.

Representative DSC thermograms are shown in Figure 8. Transition temperatures and enthalpies are listed in Table 2. The LC block **B′** in the diblock copolymer crystallizes at room temperature after a long annealing time and its melting point is 55.8 °C, while the LC block **B** in the triblock copolymer does not crystallize and the nematic structure is maintained below the T_g. Two T_g values were measured for the block copolymers: one for the LC block ($T_{gB} \approx 25$ °C, $T_{gB'} \approx 34$ °C) and another for the Iso block poly(*n*-butyl acrylate) ($T_{gA} \approx -47$ °C). The LC blocks in the two LC/Iso block copolymers exhibit the same phase sequence as the corresponding LC homopolymers, i.e., the nematic−isotropic phase sequence. For the triblock copolymer **ABA**, the nematic−isotropic transition temperature is depressed by about 25 °C relative to that of the LC homopolymer and the normalized clearing enthalpy of the LC block is about 30−40% lower than the clearing enthalpy of the LC homopolymer. These phenomena have already been reported for other LC/Iso block copolymers.[16,18,37] The decrease of the transition enthalpy is attributed to a partial isotropization of the LC subphase in vicinity of the interface between the isotropic and the LC microphase. Disordered LC polymer in the interfacial area between the domains reduces the mass of actual LC material involved in the thermal transition. Note that in the triblock copolymer discussed here the backbone structure is the same for LC and Iso blocks; both are polyacrylates. Thus, upon heating the two blocks become less and less incompatible and the poorly ordered LC interfacial area becomes larger. This also results in the wide nematic−isotropic transition range observed in the DSC curve and the depression of the clearing temperature related to the LC homopolymer. The supramolecular lamellar morphology disappears at the same time the nematic−isotropic transition occurs. In other words, the supramolecular order−disorder transformation is induced by the nematic−isotropic phase transition.

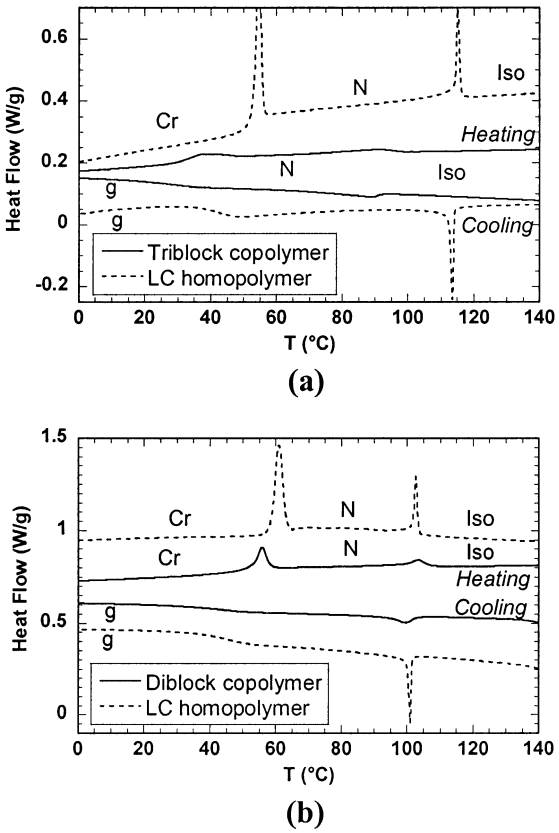

Figure 8. DSC thermograms: (a) of the triblock copolymer **ABA** and the LC homopolymer **PA444** (**B**); (b) of the diblock copolymer **AB′** and the LC homopolymer **PNB444** (**B′**). Heating/cooling rates: 10 °C·min^{-1}, second heating scan after annealing at room temperature.

The situation for the diblock copolymer **AB′** is quite different. The nematic−isotropic transition temperature and enthalpy remain, within experimental error, the same as those of the LC homopolymer. The lamellar structure persists when the LC block becomes isotropic. The X-ray results discussed in the next paragraphs support this point; the textures of the two lamellar structures are visible near the transition temperature (Figure 5b). Here, the backbone structure of the LC block, polynorbornene, is rather different from the polyacrylate Iso block. Thus, the system is strongly segregated and the interface between LC and Iso domains is apparently sharp. At high temperature, $T > T_{NI}$, , the diblock copolymer is a classical block copolymer with incompatible blocks. At the nematic−isotropic phase transition of the LC block, a lamellar−lamellar transformation is observed in the diblock copolymer.

SAXS measurements were performed on powder samples as a function of temperature. X-ray patterns exhibit typical harmonic diffraction rings. The first-order peak is first analyzed. Figures 9−11 show, respectively, the lamella spacing, the integrated intensity of the peak and the peak half-width at half-maximum (HWHM) as a function of temperature for the triblock copolymer **ABA**. Figure 9 shows a continuous decrease of the lamella thickness from 16.7 to 14.0 nm upon heating in the nematic phase of the **B** block (16% within 50 °C). There is an acceleration of the decrease near the

Table 2. Transition Temperatures (°C) and Enthalpies (in Parentheses) (J·g^{-1}) Obtained by DSC Analysis at 10 °C·min^{-1}

polymer		T_g (°C)[a] (Iso block)	T(Cr−N)[b] or T_g (°C) (LC polymer or block)	T(N−I)[b] (°C)
PA444	heating		54.6 (6.99)	115.1 (2.15)
	cooling		41	113.5 (−2.51)
PBA-*b*-PA444-*b*-PBA	heating	−47	31	91.3 (1.55)[c]
	cooling		23	89.2 (−1.45)[c]
PNB444	heating		60.9 (8.48)	102.5 (2.24)
	cooling		43	101.0 (−2.36)
PNB444-*b*-PBA	heating	−46	55.8 (3.15)	103.3 (1.97)[c]
	cooling		34	99.5 (−2.14)[c]

[a] T_g of the Iso block on cooling was not measured because it was out of the measurement limit of apparatus. [b] T(Cr−N) and T(N−I) were taken as peak temperatures in DSC thermogram. [c] The transition enthalpy for the block copolymer is scaled to the absolute amount of LC polymer.

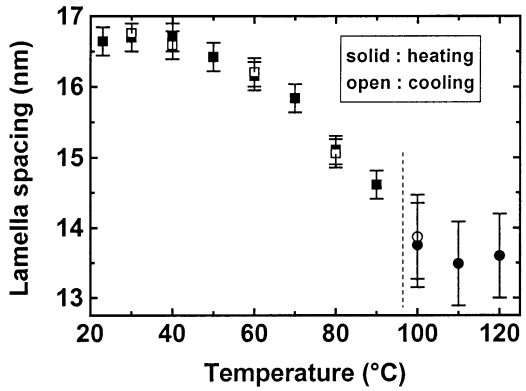

Figure 9. Lamella spacing in the supramolecular lamellar structure of the triblock copolymer **ABA** as a function of temperature. The vertical dotted line indicates the nematic−isotropic transition of the LC block.

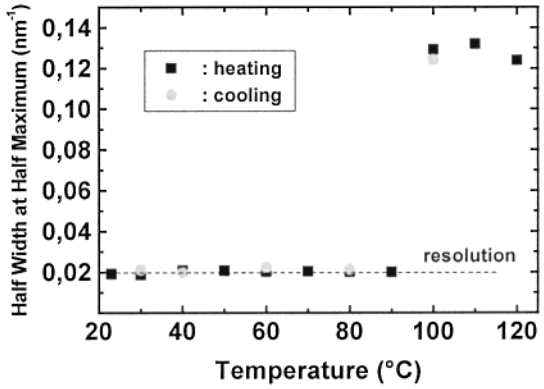

Figure 11. Half-width at half-maximum (HWHM) of the first-order X-ray diffraction peak of the triblock copolymer **ABA** as a function of temperature.

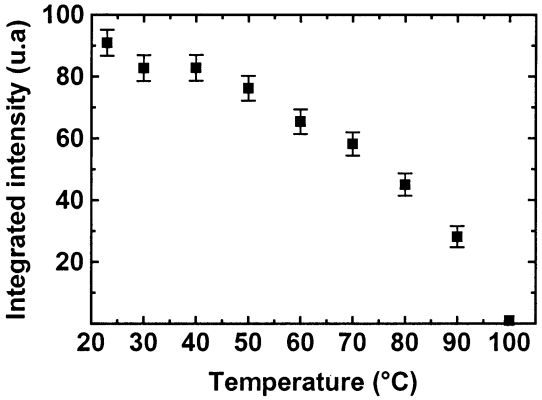

Figure 10. Integrated intensity of the first-order X-ray diffraction peak of the triblock copolymer **ABA** as a function of temperature.

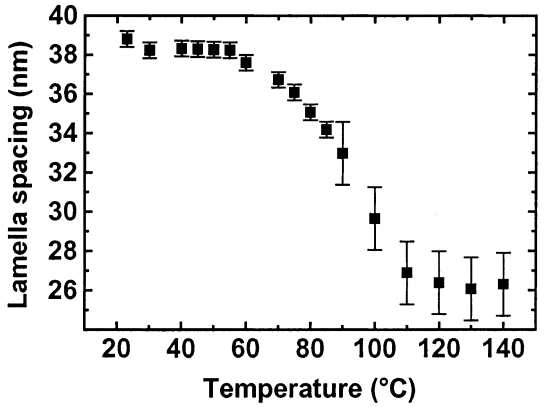

Figure 12. Lamella spacing in the supramolecular lamellar structure of the diblock copolymer **AB′** as a function of temperature.

clearing temperature, with the lamella spacing decreasing by 1 nm (6.8%) within 10 °C. This change is completely reversible on heating and cooling cycles. From Figures 10 and 11, the disappearance of the lamellar structure is clearly demonstrated at the temperature near the clearing point of the LC block. Below this temperature, the correlation length of the lamellar structure is deduced from the peak HWHM. Indeed, the peak HWHM corresponds to the apparatus resolution (2×10^{-2} nm^{-1}), which indicates a correlation length of ≥300 nm.

Figures 12 and 13 show, respectively, the lamella thickness and the integrated intensity of the peak as a function of temperature for the diblock copolymer **AB′**. There is also a continuous decrease of the lamella spacing from 38.5 to 27.0 nm upon heating in the nematic phase of the **B′** block (30% within 50 °C). The decrease accelerates also near the clearing temperature, with the lamella spacing decreasing by 2.6 nm (8.8%) within 10 °C. After the B′ block becomes isotropic, the lamella spacing remains constant at around 26.0−27.0 nm. As is the preceding case, the HWHM of the peak corresponds to the apparatus resolution over the whole temperature range. The correlation length of the lamellar structure is thus ≥ 300 nm in the whole temperature range. The supramolecular structure of the triblock and diblock copolymers can be illustrated by Figure 14.

A neutron scattering study on the LC homopolyacrylate **B** (**PA444**)[4] showed that there is a strong coupling between the nematic order of the mesogen and the backbone chain conformation. The chain conformation is strongly anisotropic at low temperature in the nematic phase; this anisotropy decreases with increasing temperature. For a sample with $DP_n = 80$, a value of $R_{\parallel}/R_{\perp} = 6$ was measured at $T = 55$ °C, and $R_{\parallel}/R_{\perp} = 3.4$

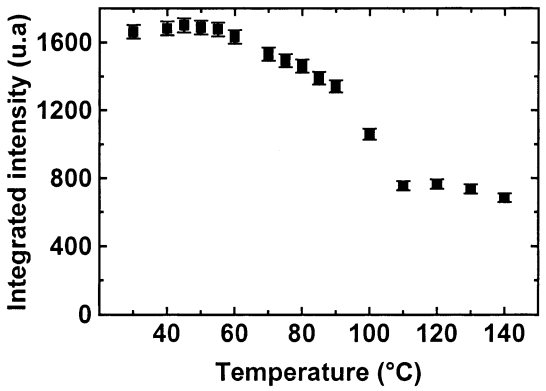

Figure 13. Integrated intensity of the first-order X-ray diffraction peak of the diblock copolymer **AB′** as a function of temperature.

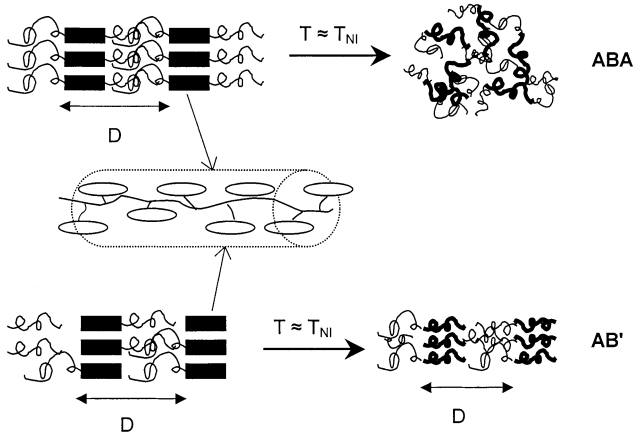

Figure 14. Schematic representation of the supramolecular lamellar structures of the triblock copolymer **ABA** and the diblock copolymer **AB′**. *D* is the lamellar thickness measured by SAXS. T_{NI} is the nematic−isotropic transition temperature of the LC block.

at $T = 105$ °C, $R_{||}$ and $R_{\perp}$ being, respectively, the radius of gyration of the polymer backbone parallel and perpendicular to the nematic director.[4] Therefore, in the supramolecular lamellar structure of the triblock copolymer, the backbone of the **B** block should also be strongly extended in the nematic phase along the direction of the layer normal. Upon heating in the nematic phase, the anisotropy of the main-chain conformation should decrease as in the case of the homopolymer. This may explain why the lamella spacing decreases upon heating. Even though the conformation of the LC polynorbornene **B′** (**PNB444**) was not studied, we expect that its conformational behavior is similar to that of the polyacrylate **B**. The decrease of lamella spacing upon heating would therefore also result from the decrease of the main-chain conformational anisotropy. At the nematic−isotropic phase transition, the main-chain conformation changes from being rather extended to a random-coil. A steep decrease of lamella spacing takes place. However, the extent of this jump is different for the triblock copolymer and for the diblock copolymer. This may be explained by the difference in the LC block chain length ($DP_{\mathbf{B}} = 24$, while $DP_{\mathbf{B'}} = 33$), since $R_{||}/R_{iso}$ depends on the degree of polymerization (R_{iso} is the radius of gyration of the LC block in the isotropic phase). It may also be related to the weak nematic order parameter found in the triblock copolymer, which is due to a large interfacial effect between the N and Iso blocks made of the same acrylate species. A similar temperature dependence of the lamella spacing has also been reported in a diblock copolymer in which the LC segment forms smectic A phase, which was also attributed to a conformational change of the main-chain backbone.[12]

Summary

Atom transfer radical polymerization and ring opening metathesis polymerization were successfully used to prepare side-on liquid crystalline polymers **PA444** and **PNB444** with unimodal molecular mass distributions of about 1.1. The two polymers exhibit crystal, N and isotropic phases. A triblock copolymer and a diblock copolymer with amorphous poly(*n*-butyl acrylate) were also prepared by ATRP using **PA444** and **PNB444** as macroinitiators. They have rather well-defined structures with unimodal distributions around 1.3. These block copolymers generate lamellar types of microphase separation. The LC block in its microphase exhibits nematic−isotropic transition similar to that of the homopolymer. For the triblock copolymer, a supramolecular order−disorder transition is induced by the nematic−isotropic phase transition of the LC block and the nematic−isotropic transition temperature is depressed by 25 °C relative to that of the homopolymer. For the diblock copolymer, the lamellar structure persists when the LC block becomes isotropic and the nematic−isotropic transition temperature remains the same as that of the homopolymer. An important structural characteristic in these microphase segregated systems is that the lamella spacing decreases significantly through transitions from the glassy or crystal to isotropic phase after a continuous shrinking over the all nematic range and a steep decrease at the nematic−isotropic transition. This decrease of spacing will be the motor of contraction of an artificial muscle prepared with the triblock copolymer. To obtain uniaxial contraction of the material, we need to obtain a monodomain of the lamellar structure in which the nematic sublayer is also well aligned. The X-ray scattering experiments of the sample aligned by a magnetic field (1.7 T) showed that the supramolecular lamella were well oriented, but the alignment of the nematic phase in the LC sublayer was not very good. Investigations are underway to improve the nematic alignment. Work is also in progress in order to prepare triblock copolymers of **PBA-*b*-PNB444-*b*-PBA** type and triblock copolymers that are cross-linkable in the amorphous part.

Acknowledgment. The authors thank Monique Mauzac and Patrick Davidson for helpful discussions.

Supporting Information Available: Text giving details of the evaluation of the M_w/M_n value of block copolymers using conventional calibration method with polystyrene standard, and a figure showing nematic phase textures of LC homopolymers **PA444** and **PNB444** under a polarizing microscope. This material is available free of charge via the Internet at http://pubs.acs.org.

References and Notes

(1) de Gennes, P.-G. *C. R. Acad. Sci. Paris* **1997**, *324* (*IIb*), 343.
(2) D'Allest, J. F.; Maissa, P.; tenBosch, A.; Sixou, P.; Blumstein, A.; Blumstein, R.; Teixeira, J.; Noirez, L. *Phys. Rev. Lett.* **1988**, *61*, 2562.
(3) Li, M.-H.; Brûlet, A.; Davidson, P.; Keller, P.; Cotton, J.-P. *Phys. Rev. Lett.* **1993**, *70*, 2297.
(4) Leroux, N.; Keller, P.; Achard, M. F.; Noirez, L.; Hardouin, F. *J. Phys. II* **1993**, *3*, 1289.

(5) Leroux, N.; Achard, M. F.; Keller, P.; Hardouin, F. *Liq. Cryst.* **1994**, *16*, 1073.
(6) Thomsen, D. L., III; Keller, P.; Naciri, J.; Pink, R.; Jeon, H.; Shenoy, D.; Ratna, B. R. *Macromolecules* **2001**, *34*, 5868.
(7) Walther, M.; Finkelmann, H. *Prog. Polym. Sci.* **1996**, *21*, 951.
(8) Fischer, H.; Poser, S. *Acta Polym.* **1996**, *47*, 413.
(9) Poser, S.; Fischer, H.; Arnold, M. *Prog. Polym. Sci.* **1998**, *23*, 1337.
(10) Pugh, C.; Kiste, A. L. *Prog. Polym. Sci.* **1997**, *22*, 601.
(11) Bohnert, R.; Finkelmann, H. *Macromol. Chem. Phys.* **1994**, *195*, 689.
(12) Yamada, M.; Iguchi, T.; Hirao, A.; Nakahama, S.; Watanabe, J. *Macromolecules* **1995**, *28*, 50.
(13) Yamada, M.; Itoh, T.; Nagagawa, R.; Hirao, A.; Nakahama, S.; Watanabe, J. *Macromolecules* **1999**, *32*, 282.
(14) Zheng, W. Y.; Hammond, P. T. *Macromol. Rapid Commun.* **1996**, *17*, 813.
(15) Omenat, A.; Lub, J. *Chem. Mater.* **1998**, *10*, 518.
(16) Komiya, Z.; Schrock, R. R. *Macromolecules* **1993**, *26*, 1387.
(17) Hefft, M.; Springer, J. *Macromol. Rapid Commun.* **1990**, *11*, 397.
(18) Adams, J.; Gronski, W. *Macromol. Rapid Commun.* **1989**, *10*, 553.
(19) Sänger, J.; Gronski, W. *Macromol. Chem. Phys.* **1998**, *199*, 555.
(20) Fischer, H.; Poser, S.; Arnold, M. *Macromolecules* **1995**, *28*, 6957.
(21) Mao, G.; Wang, J.; Clingman, S. R.; Ober, C. K. *Macromolecules* **1997**, *30*, 2556.
(22) Moment, A.; Miranda, R.; Hammond, P. T. *Macromol. Rapid Commun.* **1998**, *19*, 573.
(23) Wan, X.-H.; Tu, Y.-F.; Zhang, D.; Zhou, Q.-F. *Chin. J. Polym. Sci.* **1998**, *16*, 377.
(24) Barbosa, C. A.; Gomes, A. S. *Polym. Bull. (Berlin)* **1998**, *41*, 15.
(25) Pragliola, S.; Ober, C. K.; Mather, P. T.; Joen, H. G. *Macromol. Chem. Phys.* **1999**, *200*, 2338.
(26) Kasko, A. M.; Heintz, A. M.; Pugh, C. *Macromolecules* **1998**, *31*, 256.
(27) Chang, C.; Pugh, C. *Macromolecules* **2001**, *34*, 2027.
(28) Kasko, A. M.; Grunwald, S. R.; Pugh, C. *Macromolecules* **2002**, *35*, 5466.
(29) Li, M.-H.; Keller, P.; Grelet, E.; Auroy, P. *Macrom. Chem. Phys.* **2002**, *203*, 619.
(30) Keller, R. N.; Wycoff, H. D. *Inorg. Synth.* **1946**, *2*, 1.
(31) Percec, V.; Barboiu, B.; Kim, H.-J. *J. Am. Chem. Soc.* **1998**, *120*, 305.
(32) Garelli, N.; Vierling, P. *J. Org. Chem.* **1992**, *57*, 3046.
(33) Keller, P.; Thomsen, D. L., III; Li, M.-H. *Macromolecules* **2002**, *35*, 581.
(34) Davis, K. A.; Matyjaszewski, K. *Macromolecules* **2000**, *33*, 4039.
(35) Software documents for the miniDAWN light-scattering instrument, Wyatt Technology Corp., Santa Barbara, CA, 1998.
(36) Davidson, P.; Petermann, D.; Levelut, A. M. *J. Phys. II* **1995**, *5*, 113.
(37) Fischer, H.; Poser, S.; Arnold, M.; Frank, W. *Macromolecules* **1994**, *27*, 7133.

MA021473O